Journal of Advanced Electrochemistry 2(4) (2016) 136–140

ISSN: 2455-0205

Contents List available at JACS Directory

Journal of Advanced Electrochemistry

journal homepage: http://www.jacsdirectory.com/jaec

A Study of the Corrosion Performance of Aluminum Alloy 7075T6 in Various Superficial and Conducting Polymer Coating Conditions for Aerospace Applications

I. Pereyra[1], M. Nicho[1], A.M. Ramirez-Arteaga[1, 2], E.F. Diaz[1, 2], E. Valenzuela[3], S. Serna[1,*]

[1]*Centro de Investigación en Ingeniería y Ciencias Aplicadas - UAEM, Av. Universidad 1001, Chamilpa 62209, Cuernavaca Morelos, México.*
[2]*Facultad de Ciencias Químicas e Ingeniería, Programa Educativo de Ingeniería Mecánica-UAEM, Chamilpa 62209, Cuernavaca Morelos, México.*
[3]*Facultad de Ingeniería, UA Mexicali, lvd. enito u re calle de la Normal ol. Insurgentes Este, 2 280, México.*

ARTICLE DETAILS

Article history:
Received 22 October 2016
Accepted 12 November 2016
Available online 27 December 2016

Keywords:
Semiconductor Polymer Coatings
Superficial Treatments
Aluminum Alloy

ABSTRACT

In this work several superficial conditions of aluminum alloy T6 were study in NaCl solution with and without conductor polymer (CP) coating P3OT (poly (3-octyl thiophene) for corrosion resistant in aerospace applications. The results show that the aluminum the anodized condition and aluminum alloy T6 deprived of any coating and superficial treatment shows the worst corrosion performance. On the other wat aluminum samples anodized plus P3OT coating gives the better corrosion rates but aluminum alloys and P3OT are also a good option for preventing corrosion in NaCl environment.

1. Introduction

The corrosion of aluminum alloys is multifaceted, includes many issues, and differs rendering to metal and precise operating conditions. So far all remain difficult to regulate, and signify a very dangerous risk to most factories. Once recognized, most corrosion difficulties will produce years of operating trouble and expenses.

To generate wanted, useful and decorative features and stuff, anodizing aluminum alloys is an extensive technique used for corrosion protection, adhesion promotion and wear resistance [1]. A vast number of methods are known used in various branches of industry. Classified mainly by their electrolyte composition, the temperature, the voltage and the type of current) used to produce these features. The most usual techniques employ electrolytes based on sulphuric acid.

High strength aluminum alloys such as Al–Zn–Mg alloys are highly important materials in aircraft industries, these alloys are formed by a very heterogeneous microstructure, which is of Al solid solutions matrix with various intermetallic phases. The importance of this microstructure and the influence of the intermetallic on the corrosion behavior were intensively discussed in the literature [2-12]. The intermetallic enhanced the different local corrosion processes such as pitting corrosion, crevice corrosion or intergranular corrosion, because a galvanic coupling between the intermetallic and the aluminum matrix exists. Thus, intermetallic could be more or less nobles than the matrix, these also play a significant role, understanding the protection mechanism of inhibitors and conversion coatings.

On the other hand, conducting polymer (CP) coatings has been used for corrosion protection during past years on carbon and stainless steel, due to the presence of heteroatoms and/or pi-electrons in their molecules in addition to availability, cost effectiveness, and eco-friendliness. Leading improved corrosion performance by the formation of a steady passive oxide film between the polymer and steel, a barrier effected by corrosive ions and electro active interactions of adhesive polymer layer with corrosive ions [13-22]. The potentials of several CPs are positive relative to iron and aluminum, so, they should deliver anodic protection effects comparable to those provided by the passivating oxides of iron and similar inorganic systems. CPs placed on metals surfaces have been established to stabilize a fixed potential inside passive range and to block the access of aggressive anions (e.g. chlorides to substrate) [23]. Furthermore, CPs protect the metal too by producing anodic shift in the corrosion potential as they are galvanic ally couple to the metal [24, 25].

There are numerous means frequently used to fight aluminum alloy corrosion. These include passive film formation, chromatin, cathodic protection, organic coatings and inhibitors. The aim of this work is to study the corrosion protection of aluminum alloy 7075-T6 with and without anodizing conditions and the addition of conducting polymer P3OT (synthesized by the chemical polymerization technique) and deposited by the drop-casting technique a very cheap technique for industrial application evaluated in NaCl solution.

2. Experimental Methods

2.1 Materials

Material used as substrate was commercial aluminum alloy 7075-T6 in coupons with 1.0 cm^2 of exposed area spot welded to a Ni–20Cr wire. The alloy chemical composition was shown in Table 1. The aluminum alloy also was solution heat treated to remove the precipitation originated by the T6 condition.

Table 1 Chemical composition of alloy AA7075-T6

%	Si	Fe	Cu	Mn	Mg	Cr	Zn	Ti	Al	Others
Min.			1.2		2.1	0.18	5.1		87.1	
Max.	0.4	0.5	2.0	0.3	2.9	0.28	6.1	0.2	91.4	0.15

Distilled 3-octylthiophene (3OT) monomer (Aldrich) was used for the synthesis of the polymer.

2.2 Anodizing Process

Aluminum couples were degreased using 0.5 M NaOH solution at 40 °C for 3 minutes and neutralized in HNO_3 for 30 seconds. Then aluminum alloy coupons were anodized in an electrochemical cell with H_2SO_4 at 30 % in volume, using 10 V for 30 minutes. Stainless steel 304 was used as counter electrode to close the circuit, the aluminum coupon act as the anode. Finally, the aluminum coupon surface was sealed by immersion in distilled water for 30 seconds, only analytic grade reagents were used for preparing the solutions.

*Corresponding Author
Email Address: aserna@uaem.mx (S. Serna)

Cite this Article as: I. Pereyra, M. Nicho, A.M. Ramirez-Arteaga, E.F. Diaz, E. Valenzuela, S. Serna, A study of the corrosion performance of aluminum alloy 7075T6 in various superficial and conducting polymer coating conditions for aerospace applications, J. Adv. Electrochem. 2(4) (2016) 136–140.

2.3 P3OT Chemical Synthesis

Poly(3-octyl thiophene), P3OT, was obtained by the oxidative polymerization of 3-octyl thiophene, 3OT, with $FeCl_3$ as oxidant [26]. Three mixtures were prepared: (a) A mixture with anhydrous $FeCl_3$ (6.22 g) and $CHCl_3$ (207.33 mL) and (b) a mixture with 3OT (5.43 mL) and $CHCl_3$ (62.17 mL). Both mixtures were prepared in an inert atmosphere. (c) The reaction mixture (a+b) was stirred at room temperature during 25 h. The product was precipitated in methanol (800 mL), filtered with a Buchner funnel and carefully washed with methanol, hydrochloric acid (10%vol.), acetone, NH_4OH (10 vol.%), ethylenediaminetetraacetic acid (EDTA, 1 vol.%) and distilled water. The final black P3OT product was then dried at 55 °C during 12 hrs. Analytic grade reagents were used for preparing the solutions.

2.4 Deposition Process

P3OT coatings were deposited onto aluminum 7075 samples by the drop casting technique. This technique consists in the deposition of 12 drops as standard measurement of polymeric solution (P3OT in toluene, in a concentration of 6.6 to 10.2 g/L) on the substrate and once the solvent has been evaporated, the film is obtained [20].

The polymeric solution was dried within a chamber in a saturated atmosphere of toluene. Before the deposition process, aluminum alloy substrates were abraded with 1200 grade emery paper and polished with 1.0-micron alumina particles and finally washed with water and degreased with ethyl alcohol.

2.5 Characterization of P3OT

The number average (Mn) and weight average (Mw) molecular weights and polydispersity (PD) were determined by a size exclusion chromatograph (SEC, Hewlett Packard HPLC 1100) equipped with in line vacuum degasser, auto sampler and UV detector. The SEC equipment was fitted with three PLgel 5-10 mm columns (pore size 106, 105, 103; 300 mm x 7.5 mm) and one PL gel 10 mm guard column (50 mm x 7.5 mm) (Polymer Laboratories) and operated using tetrahydrofuran as eluent at 1.0 mL/min at 40 °C. Molecular weights are expressed as polystyrene equivalents (standards 1x106-400 Da).

The instrument was calibrated with polystyrene standards. Dyads configuration was determined by ^1H NMR (Varian Inova 400 instrument) using $CHCl_3$ as solvent. The dyads (HH and HT) contents in P3OT polymer were estimated from the peak areas that appeared around δ = 2.55 (HH), 2.8 (HT) [27]. The thermal stability and decomposition temperature of the polymers were determined by Thermogravimetric analysis (TGA TA Q500), the samples were heated at 10 °C/min rate under nitrogen atmosphere. Fourier transform infrared spectroscopy (FTIR) spectra of samples were recorded in a FT-IR Spectrometer GX, Perkin Elmer.

2.6 Corrosion Tests

NaCl saturated solution was prepared with analytical grade chemical reagents. Potentiodynamic polarization curves were carried out by using a potentiostat controlled by a computer at a scan rate of 1 mV/s in a three-electrode electrochemical cell with a saturated silver/silver chloride (Ag/AgCl) electrode as reference electrode and a graphite rod as auxiliary electrode.

Electrochemical impedance spectroscopy (EIS) tests were carried out at E_{corr} by using a signal with amplitude of 10 mV vs Ag/AgCl and a frequency interval of 0.1 Hz-30 kHz. A model PC4 300 Gamry potentiostat was used for this. Finally, surface morphology of the polymer covered aluminum samples, before and after corrosion tests were analyzed in a scanning electron microscope (SEM, Karl Seizz DSM100).

3. Results and Discussion

3.1 Microstructure

The as received commercial alloy 7075-T6 contains various other elements and impurities (Table 1), all these take part on microstructure formation. This alloy not be could described as ternary phase system. Due to the partial solubility of these elements in aluminum, a number of intermetallic will develop resulting in a heterogeneous microstructure. The intermetallic phases could be evolved by two different ways: 1) during solidification from the melt and 2) by a successive heat treatment, solution annealing or age hardening. The different kind of intermetallic will control the anodizing process. The straight oxidation of aluminum to alumina, is accompanied by the creation of oxide films affording to $2Al + 3H_2O \rightarrow Al_2O_3 + 3H_2$ especially in the early stage of anodizing.

Fig. 1 shows light microscopic images of the T6 sample in the normal rolling direction, many precipitations were observed within the aluminum granular matrix pancake microstructure, the types of intermetallic can be found in the literature. The process of phase formation is not only determined by thermodynamic aspects but also by kinetics during production and treatments. According to Tallman [24] the dark particles in Fig. 1 were interpreted as η' f fine size precipitates (Fig. 1b) highly density observed. Fig. 1c show a EDX taken at the yellow arrow showing that this precipitates contain Al-Mg-Zn. Fig. 2 shows the aluminum alloy in solubilized condition as seen almost any precipitate was removed and only is revealed a very few precipitates in the granular pancake matrix microstructure.

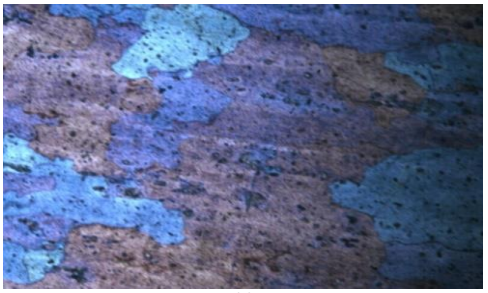

(a)

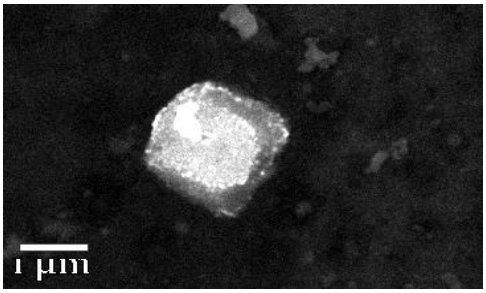

(b)

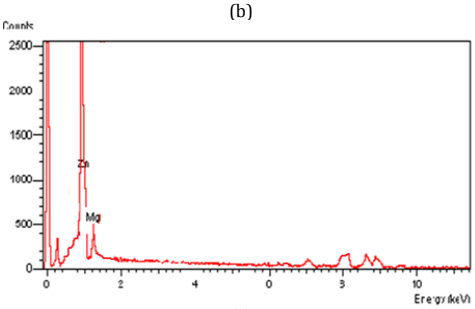

(c)

Fig. 1 Aluminum 7075 (20X) (a) Aluminum pancake microstructure with dense precipitation (b) η' fine size precipitate (c) EDX of precipitate chemical composition (Al-Mg-Zn)

Fig. 2 Aluminum 7075 (20X) with almost any precipitation

3.2 P3OT Characterization

The P3OT product showed Mn= 42,359 g/mol, Mw = 141,258 g/mol, PDI= 3.3 estimated by GPC in THF using polystyrene as standard. The structural regularity of the P3OT polymer was examined by ^1H NMR spectroscopy (not shown spectrum). The spectra showed two peaks in the 2.4-2.9 ppm region (2.54 ppm and 2.78 ppm), due to the α-CH_2 protons that is directly connected to the thiophene ring. The signal at 2.78 ppm corresponds to head-to-tail (HT) and that of 2.54 ppm to head-to-head (HH) configuration of dyads. The dyads contents of P3OT polymers were 76% of HT and 24% off HH.

Cite this Article as: I. Pereyra, M. Nicho, A.M. Ramirez-Arteaga, E.F. Diaz, E. Valenzuela, S. Serna, A study of the corrosion performance of aluminum alloy 7075T6 in various superficial and conducting polymer coating conditions for aerospace applications, J. Adv. Electrochem. 2(4) (2016) 136–140.

Fig. 3 shows the FTIR spectrum of P3OT. The characteristic bands of P3OT polymer were observed: three bands at 2956, 2921 and 2849 cm^{-1} (stretching C-H aliphatic, which have been assigned respectively to the asymmetric C-H stretching vibrations of $-CH_3$ moieties, $-CH_2-$ moieties, and symmetric C-H stretching vibration in $-CH_2-$ moieties). The two bands at 1456 and 1506 cm^{-1} (aromatic C=C stretching, symmetric and asymmetric) are characteristic of the 2,3,5-trisubstituted thiophene ring. The band at 1379 cm^{-1} corresponds to the methyl bending. The band at 826 cm^{-1} to the aromatic C-H out-of plane vibration of a 2,3,5-trisubstituted ring and the band at 718 cm^{-1} at rocking vibration of hexyl substituent methylene groups $-(CH_2)_5-$) [28].

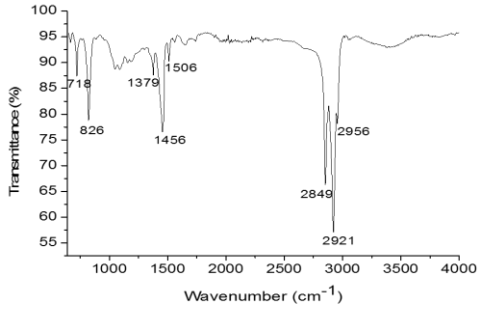

Fig. 3 FTIR spectra in the frequency rangen (640–4000 cm^{-1}) of P3OT polymer

TGA spectrum of P3OT polymer is shown in Fig. 4. The results showed the P3OT decomposition temperature at 480 °C and stability until approximately 200 °C.

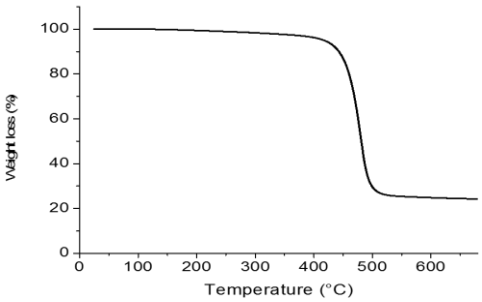

Fig. 4 TGA spectrum of P3OT polymer

3.3 Adhesion Test

According to the ASTM 3359 norm, the adherence is measured as 0B, 1B, 2B, 3B, and 4B, where 0B describes coatings with weak adherence and 4B describes those with high adherence. The polymeric coatings showed good adherence, between 2B and 3B.

3.4 Polarization Curves

In Fig. 5 we can see the Polarization curves of all the samples studied, T6 (S) condition and solubilized plus anodized (SA) samples show very similar behaviors, illustrated by their polarization curves. These curves show active passivating and trans passive zones in the anodic part and limit current (i_{lim}) in the cathodic part (Table 2). When the substrate was coated, the E_{corr} values were shifted in the noble direction.

The solubilized plus anodized plus polymer (SAP) and the solubilized plus polymer (SP) (polarization curves respectively, present continuous anodic dissolution at any potential but also show much more less corrosion rates (i_{corr}) until three or four order of magnitude. The E_{corr} and I_{corr} values were calculated by Tafel extrapolation. The results are summarized in Table 2.

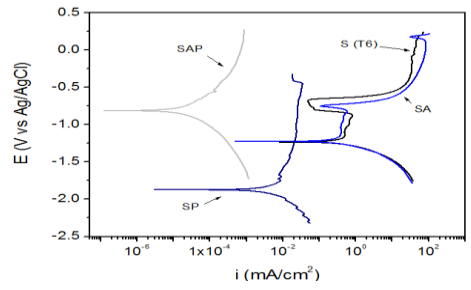

Fig. 5 Polarization curves for the AA7075 alloy, referred to as T6, with and without anodizing conditions and the addition of conducting polymer P3OT in 0.5 M NaCl solution

Table 2 Corrosion parameters from PC obtained from Fig. 3

Treatment	E_{corr} (V)	I_{corr} (mA/cm²)
T6 Solubilized (S)	-1.180	0.262
Solubilized + Anodized (SA)	-1.205	0.322
Solubilized + Polymer (SP)	-1.886	0.001
Solubilized + Anodized + P (SAP)	-0.812	1.452×10^{-5}

The solution plus anodized plus polymer as the solution plus polymer condition surface are capable to protect in a more efficient way their surfaces than aluminum alloy 7075-T6 surface and aluminum alloy plus solution treated plus anodized surfaces, besides they can suffer pitting as seen on their respective curves. To analyze well their corrosion mechanisms, EIS test has been carried out.

3.5 Electrochemical Impedance Spectroscopy (EIS)

Intermetallic particles which play a cathodic role in aluminum alloys cause depolarizing behaviors, initiating pitting in aluminum- alloys, the polarization curve of the T6 condition as the solubilized plus anodized surface shows pitting. This is being reported in the literature [29, 30], where oxygen reduction occurs as cathodic reaction on intermetallic particles. Anodic reaction is needed for the development of passive layer on the matrix. Then, intermetallic oxygen reduction, movement of Al^{+3} ions over the passive layer and consequent passive layer thickening are the foremost processes, which occur to T6 and solubilized plus anodized samples [31]. Accordingly, exist three elements that play for pitting corrosion of these samples: substrate-passive layer interface, sole passive layer and intermetallic particle.

These scenarios could be could be described by the equivalent circuit shown in Fig. 4,

where,

R_s: uncompensated resistance among working and reference electrode.
R_{int}: resistance from intermetallic particles.
C_{int}: capacitance from intermetallic particles.
R_{np}: passive layer resistance.
CPE_n: constant phase element in passive layer.
R_{ct}: charge transfer resistance at substrate-passive layer interface.
CPE_{dl}: double layer constant phase element in substrate-passive layer interface.

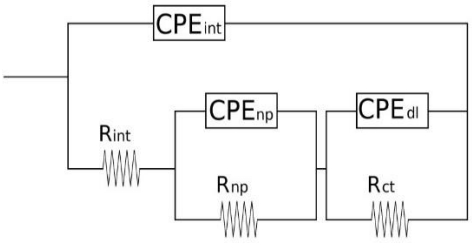

Fig. 6 Equivalent circuit obtained for the T6 sample at the 5 h nyquist plot

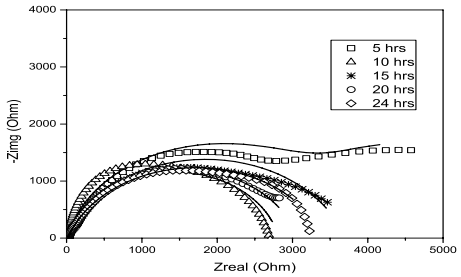

Fig. 7 Impedance diagrams obtained for the T6 samples

Table 3 Electrical parameter values for the T6 electrode

Time (h)	R_1	CPE_{int} (x 10^{-5})	N_{int}	R_{int}	CPE_{np}	N_{np}	R_{np}	CPE_{dl} (x 10^{-5})	N_{dl}	R_{ct}
5	1	5.21	0.88	4000	5.00×10^{-6}	0.60	2300	100	1.00	6301
10	90	5.00	0.85	2600	1.00×10^{-5}	1.00	120	1	1.00	2810
15	90	5.00	0.85	400	1.00×10^{-5}	0.70	3200	1	0.70	3690
20	50	10.0	0.85	2950	1.00×10^{-6}	0.80	50	1	1.00	3050
24	50	10.0	0.80	3000	1.00×10^{-5}	0.80	350	10	0.80	3400

Fig. 7 and Table 3 shows EIS results showing Nyquist plots of aluminum samples, for the T6 condition surface. The T6 sample is not solution treated, so a variety of particles could be seen on its surface (Fig. 1).

Among aluminum alloy matrix and intermetallic particles, a galvanic cell form, leading to a local increase in the pH, permitting, the dissolution of the oxide layer in the area neighboring the intermetallic particle. When the layer has been dissolved, the local alkalinity makes possible a penetrating attack on the matrix particle interface, and particle detachment made the pit (plot at 10 h) plot. Then, at high frequencies can be observed the response of passive layer on intermetallic particles perturbation (15 h plot). At somewhat stumpy frequencies the reply related with passive layer -substrate interface will be detected than the localized alkaline corrosion process. At last in the low frequency series, the Al^{+3} transport through the passive layer, one of the slow system process, is finally showed (plots at 20 and 24 h) [31, 32].

For Nyquist plots the equivalent circuit in Fig. 6 can serve to simulate models for their corresponding plots. aluminum alloys pitting generates uniformities and roughness in its surface, leading unideal capacitor performance and Nyquist plot depression [33, 34]. So, constant phase element (CPE), replace capacitance in equivalent circuits. It is seen that there is a good agreement between the experimental and simulated data.

On the other hand, all the other samples exhibited a behavior typical for a coated material, were a two semicircles response is clearly observed. Consequently, the equivalent circuit in Fig. 8 was substituted with the circuit shown in Fig. 6. We can explain this change because at contact initial times in intermetallic particles suffer strong cathodic activity, and two activities take place with elapsed time. Electric contact debilitation among solution and particles since corrosion sub products growth inside pits and crevice corrosion between intermetallic particles and the matrix. In both conditions, cathodic reactions on intermetallic particles become suppressed. Therefore, removal of C_{int} and R_{int} from the equivalent circuit, shown in Fig. 8.

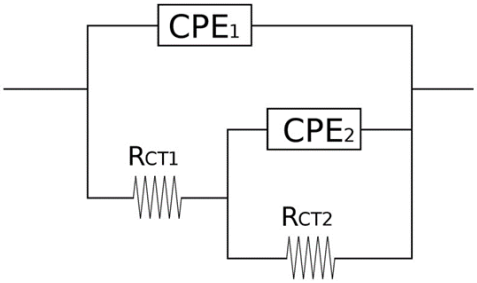

Fig. 8 The Electrical equivalent circuit used to simulate the impedance results from the SAP, SP and SA samples

It can be seen that there is good compatibility between the experimental and simulated data in Nyquist plots. (Figs. 9-11) Therefore, it is possible to interpret all variations on the sample by equivalent circuit in Fig. 8, where R_{CT1} is uncompensated resistance between working and reference electrode; CPE_1 p is constant phase element through passive layer; R_{CT2} is passive layer resistance; CPE_2 is constant phase element at substrate/passive layer interface and R_{CT1} is charge transfer resistance at substrate/passive layer interface.

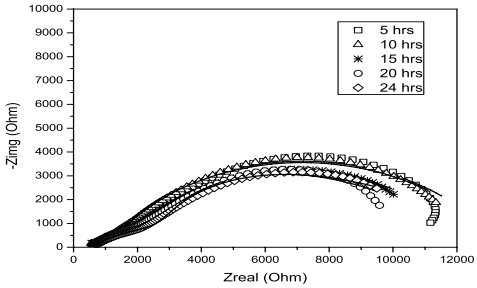

Fig. 9 Nyquist plot at different immersion times for the SAP sample

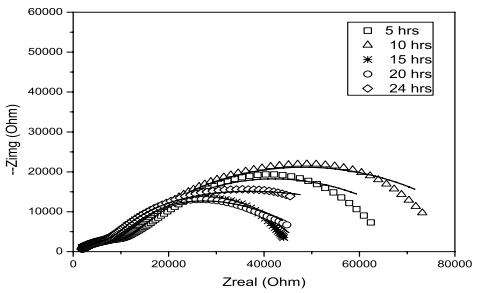

Fig. 10 EIS diagram for the SP sample

Table 4 Values for the electrical parameters obtained in the simulation for the SAP sample

Time (h)	R_1	CPE_1 (x 10^{-5})	N_1	R_2	CPE_2 (x 10^{-5})	N_2	R_{CT}
5	1000	1	0.6	12000	2	0.7	13000
10	980	1.1	0.57	12000	2.5	0.7	12980
15	2833	3.2	0.48	10000	2	0.85	12833
20	4415	4	0.46	8000	2.3	1	12415
24	4492	4.7	0.43	9000	2.21	1	13492

Table 5 Electrical parameters values for the SP Electrode

Time (h)	R_1	CPE_1 (x 10^{-6})	N_1	R_2	CPE_2 (x 10^{-6})	N_2	R_{CT}
5	16219	3.54	0.40	63672	5.50	0.74	79891
10	13610	2.45	0.46	77233	3.72	0.67	90843
15	10940	2.27	0.52	37288	2.87	0.77	48228
20	13568	5.67	0.45	39812	3.11	0.84	53380
24	19618	1.05	0.39	62086	2.30	0.88	81704

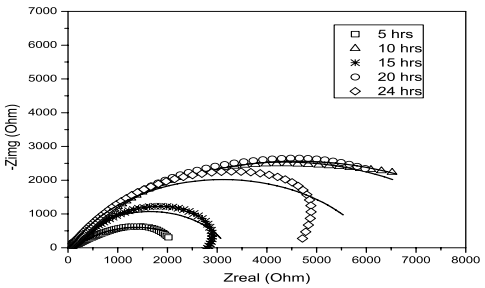

Fig. 11 Nyquist plot a different immersion times for SA electrode

Table 6 Electrical parameters value of SA electrode

Time (h)	R_1	CPE_1 (x 10^{-5})	N_1	R_2	CPE_2 (x 10^{-5})	N_2	R_{CT}
5	348.70	6.67	0.55	2228	16.68	0.60	2576.7
10	349.80	3.23	0.67	8236	3.87	0.69	8585.8
15	362.10	2.79	0.72	2839	2.27	0.82	3201.1
20	1629	7.17	0.63	7630	19.6	1.00	9259
24	290.90	2.85	0.73	5867	2.13	0.75	6157.9

Under these conditions, the high frequencies circle is attributed to the inner materials interphase, while the low frequency, larger semicircle, corresponds to the interaction between the outer passive layer and the electrolyte. Nevertheless, there are significant differences between the SAP and T6 samples compared with the SP and SA electrode. When observing the SAP and T6 diagrams, it is possible to identify a stable behavior during the 24 hrs evaluation, as can be validated in the R_{CT} values of Tables 3 and 5. This fact, suggests the formation of a steady passive layer, with no significant variations during the test. In the other hand, the SP and SA electrode, displayed important changes in the R_{CT} values, as can be seen in Tables 4 and 6. In this case, the materials surface interacts with the solution during the evaluation, and decreases its value in the first 15 hours to experiment a strengthening in the end of the test.

From the characterization Fig. 1 we can see that aluminum alloy 7075 in its T6 condition show a granular microstructure with several precipitates in grain boundaries and within the grains. The precipitates are identified as η' Alx-Mgy-Znz complex phases distribution in α-Al solid solution where corrosion mainly started. In the fully solubilized condition 7075 aluminum alloy all precipitates practically disappear The T6 condition shows the worst corrosion mode between all superficial conditions studied. This is clearly seen from the polarization curves (Fig. 2). In which the T6 condition show passive and trans passive behaviors. Similar performance was presented by the SA surface condition, both present the highest and similar corrosion rates values. This suggest that the purely anodized layer cannot protect by itself the aluminum alloy surface, even though its surface is almost free of precipitates, leading the corrosion start in some other superficial complex phase that was not affected by the solution heat treatment. The SAP condition as well as SP surface conditions, do not present passive zones but both surface conditions shows much lower corrosion rates, being the SAP surface the most protective surface condition. It seems that the union of the anodize layer with the polymer layer is more efficient to retard the corrosion beginning, isolating the aluminum alloy surface from the NaCl solution.

On the other hand, EIS results according with polarization Curves shows that the T6 surface condition present the worst scenario for the aluminum alloy corrosion. Furthermore, The EIS results permit to distinguish corrosion mechanism among the different samples conditions studied.

Cite this Article as: I. Pereyra, M. Nicho, A.M. Ramirez-Arteaga, E.F. Diaz, E. Valenzuela, S. Serna, A study of the corrosion performance of aluminum alloy 7075T6 in various superficial and conducting polymer coating conditions for aerospace applications, J. Adv. Electrochem. 2(4) (2016) 136–140.

Indeed, corrosion mechanism of sample T6 is completely different from the rest samples condition surfaces. Its surface is completely exposed to NaCl solution that in combination with intermetallic precipitates dense distributed leads to pitting propagation by the following reactions, where oxygen oxidation plus hydrogen evolution are the important processes at the intermetallic cathodes:

$$Al \longrightarrow Al^{3+} + 3e^{-} \quad (1)$$

$$Al^{3+} + 3H_2O \longrightarrow Al(OH)_3 + 3H^{+} \quad (2)$$

As a pit propagates the environment inside the pit (anode) changes. Reaction 2 indicates that the pH will decrease. To balance the positive charge produced by reaction 1 and 2, chloride ions will migrate into the pit. The resulting HCl formation inside the pit causes accelerated pit propagation. The reduction reaction will cause local alkalinisation around cathodic particles. As previously mentioned aluminum oxide is not stable in such environment, and aluminum around the particles will dissolve (alkaline pits). Etching of the aluminum matrix around the particles may detach the particles from the surface, which may repassivate the alkaline pits.

EIS results from P3OT coated samples indicate that the hybrid films (sol plus anodized plus polymer samples) provided exceptional barrier and corrosion protection in comparison with uncoated polymer aluminum alloy substrate T6 an SA samples) apparently, the order is from the worst to the best protection based on their R_{ct} values: T6, SA, SP and SAP.

4. Conclusion

The Polarization curves and EIS show agreement results that the aluminum the T6 deprived of any coating and the SA condition and aluminum alloy shows the worst corrosion performance. Nevertheless, aluminum samples anodized plus P3OT coating gives the better corrosion rates but aluminum alloys and P3OT are also a good option for preventing corrosion in NaCl environment. The T6 and solubilized conditions show passivation and repassivation behaviors but the fastest corrosion rates. Nyquist analysis show different corrosion mechanism between T6 condition and the other surface conditions, basically compared with specially with the polymer coated samples, in which different equivalent circuits were used to model EIS data related with differences in precipitation surfaces. The adhesion test show good integrity and adhesion conditions for the aluminum alloy substrate.

Acknowledgements

The authors thank Dr. Rene Guardian and I. Puente Lee for their support, also to CONACyT for the financial support given to I. Pereyra for the conclusion of its Doctoral Thesis.

References

[1] T.W. Jelinek, Oberflächenbehandlung von Aluminium, Eugen G. Leuze Verlag, D_88348 Saulgau/Württ, Neuauflage, 1997.
[2] G.S. Frankel, R.L. McCreery, Inhibition of Al alloy corrosion by chromates, Interf. Electrochem. Soc. 10 (2001) 34-39.
[3] C. Blanc, B. Lavalle, G. Mankowski, The role of precipitates enriched with copper on the susceptibility to pitting corrosion of the 2024 aluminium alloy, Corros. Sci. 39 (1997) 495-510.
[4] G.O. Ilevbar, J.R. Scully, J. Yuan, R.G. Kelly, Inhibition of pitting corrosion on aluminum alloy 2024-T3: effect of soluble chromate additions vs chromate conversion coating, Corros. 56 (2000) 227-242.
[5] P. Campestrini, E.P.M. van Westing, H.W. Van Rooijen, J.H.W. De Wit, Relation between microstructural aspects of AA2024 and its corrosion behavior investigated using AFM scanning potential technique, Corros. Sci. 42 (2000) 1853-1861.
[6] M. Kendig, S. Jeanjaquet, R. Addison, J. Waldrop, Role of hexavalent chromium in the inhibition of corrosion of aluminum alloys, Surf. Coat. Technol. 140 (2001) 58-66.
[7] Z. Szlarska-Smialowska, Pitting corrosion of aluminum, Corros. Sci. 41 (1999) 1743-1767.
[8] V. Guillaumin, G. Mankowski, Localized corrosion of 2024 T351 aluminium alloy in chloride media, Corros. Sci. 41 (1999) 421-438.
[9] J. Vander Kloet, W. Schmidt, A.W. Hassel, M. Stratmann, The role of chromate in filiform corrosion inhibition, Electrochem. Acta. 48 (2003) 1211-1222.
[10] Ch. Blanc, G. Mankowski, Pit propagation rate on the 2024 and 6065 aluminium alloys, Corros. Sci. 40 (1998) 411-429.
[11] G.S. Chen, M. Gao, R.P. Wei, Micro constituent-Induced pitting corrosion in aluminum alloy 2024-T3, Corros. 52 (1996) 8-15.
[12] P. Campestrini, H. Terryn, A. Hovestad, J.H.W. De Wit, Formation of a cerium-based conversion coating on AA2024: relationship with the microstructure, Surf. Coat. Technol. 176 (2004) 365-381.
[13] R. Vera, R. Schrebler, P. Cury, R. Del Rio, H. Homero, Corrosion protection of carbon steel and copper by polyaniline and poly (ortho-methoxyaniline) films in sodium chloride medium, Electrochemical and morphological study, J. Appl. Electrochem. 37 (2007) 457-463.
[14] S.A.M. Refaey, F. Taha, H.S. Shehata, Corrosion protection of mild steel by formation of iron oxide polybithiophene composite films, J. Appl. Electrochem. 34 (2004) 891-897.
[15] D. Kowalski, M. Ueda, T. Ohtsuka, Corrosion protection of steel by bi-layered polypyrrole doped with molybdophosphate and naphthalenedisulfonate anions, Corros. Sci. 49 (2007) 1635-1644.
[16] D. Kowalski, T. Ohtsuka, The effect of counter anions on corrosion resistance of steel covered by bi-layered polypyrrole film, Corros. Sci. 49 (2007) 3442-3452.
[17] D. Kowalski, T. Ohtsuka, The effect of ultrasonic irradiation during electropolymerization of polypyrrole on corrosion prevention of the coated steel, Corros. Sci. 50 (2008) 286-291.
[18] E. Armelina, R. Pla, F. Lies, X. Ramis, J.I. Iribaren, C. Aleman, Corrosion protection with polyaniline and polypyrrole as anticorrosive additives for epoxy paint, Corros. Sci. 50 (2008) 721-728.
[19] D.P. Lea, Y.H. Yoo, J.G. Kim, S.M. Cho, Y.K. Sno, Corrosion characteristics of polyaniline-coated 316L stainless steel in sulphuric acid containing fluoride, Corros. Sci. 51 (2009) 330-338.
[20] V. Shinde, S.R. Sainkar, P.P. Patil, Corrosion protective poly (o-toluidine) coatings on copper, Corros. Sci. 47 (2005) 1352-1369.
[21] J.I. Martins, T.C. Reis, M. Bazzaoui, E.A. Bazzaoui, L. Martins, Polypyrrole coatings as a treatment for zinc-coated steel surfaces against corrosion, Corros. Sci. 46 (2004) 2361-2381.
[22] N.D. Nam, J.G. Kim, Y.J. Lee, Y.K. Son, Effect of thermal treatment on the corrosion resistance of polyaniline in H_2SO_4-HF acid mixture solution, Corros. Sci. 51 (2009) 3007-3013.
[23] M.A. Malik, R. Włodarczyk, P.J. Kulesza, H. Bala, K. Miecznikowski, Protective properties of hexacyanoferrate containing polypyrrole films on stainless steel, Corros. Sci. 47 (2005) 771-783.
[24] D.E. Tallman, G. Spinks, A. Dominis, G. Wallace, Electroactive conducting polymers for corrosion control, J. Solid State Electrochem. 6 (2002) 73-100.
[25] Jin-feng Li, Zhuo-wei PENG, Chao-xing LI, Zi-qiao ZHENG, Mechanical properties, corrosion behaviors and microstructures of 7075 aluminium alloy with various aging treatments, Transactions of No Ferrous Metals Society of China 18 (2008) 775-762.
[26] M.E. Nicho, C.H. García-Escobar, M.C. Arenas, P. Altuzar-Coello, R. Cruz-Silva, et al, Influence of P3HT concentration on morphological, optical and electrical properties of P3HT/PS and P3HT/PMMA binary blends, Mater. Sci. Engg. B 176 (2011) 1393-1400.
[27] M. Sato, H. Morii, Nuclear magnetic resonance studies on electrochemically prepared poly (3-dodecylthiophene), Macromolecules, 24 (1991) 1196-1200.
[28] S. Hotta, S.D.D.V. Rughooputh, A.J. Heeger, F. Wudl, Spectroscopic studies of soluble poly (3-alkylthienylenes), Macromolecules 20 (1987) 212-215.
[29] N. Birbilis, R.G. Buchheit, Electrochemical characteristics of intermetallic phases in aluminum alloys an experimental survey and discussion, J. Electrochem. Soc. 152(4) (2005) B140-B151.
[30] A. Aballe, M. Bethencourt, F.J. Botana, M.J. Cano, M. Marcos, Localized alkaline corrosion of alloy AA5083 in neutral 3.5% NaCl solution, Corros. Sci. 43 (2001) 1657-1674.
[31] A. Barbucci, G. Bruzzone, M. Delucchi, M. Panizza, G. Cerisola, Breakdown of passivity of aluminium alloys by intermetallic phases in neutral chloride solution, Intermetallics 8 (2000) 305-312.
[32] H.B. Shao, J.M. Wang, Z. Zhang, Electrochemical impedance spectroscopy analysis on the electrochemical dissolution of aluminum in an alkaline solution, J. Electroanal. Chem. 549 (2003) 145-150.
[33] J.B. Jorcin, M.E. Orazem, P. Nadine, B. Tribollet, CPE analysis by local electrochemical impedance spectroscopy, Electrochem. Acta 51 (2006) 1473-1479.
[34] K. Jafarzadeh, T. Shahrabi, M.G. Hosseini, EIS study on pitting corrosion of AA5083-H321 aluminum-magnesium alloy in stagnant 3.5% NaCl solution, Mater. Sci. Technol. 24 (2008) 215-219.